

## Article

# Clinical, Cortical, Subcortical, and White Matter Features of Right Temporal Variant FTD<sup>†</sup>

Jana Kleinerova<sup>1,‡</sup>, Mary Clare McKenna<sup>1,2,‡</sup>, Martha Finnegan<sup>3</sup>, Asya Tacheva<sup>1</sup>, Angela Garcia-Gallardo<sup>2</sup>, Rayan Mohammed<sup>2</sup>, Ee Ling Tan<sup>1</sup>, Foteini Christidi<sup>1</sup>, Orla Hardiman<sup>1</sup>, Siobhan Hutchinson<sup>2</sup> and Peter Bede<sup>1,2,\*</sup>

<sup>1</sup> Computational Neuroimaging Group, School of Medicine, Trinity College Dublin, D08 W9RT Dublin, Ireland

<sup>2</sup> Department of Neurology, St James's Hospital, D08 KC95 Dublin, Ireland

<sup>3</sup> Department of Psychiatry, Tallaght University Hospital, D24 NR0A Dublin, Ireland

\* Correspondence: bedep@tcd.ie

<sup>†</sup> This is a part of Ph.D. thesis of Dr. Mary Clare McKenna.

<sup>‡</sup> These authors contributed equally to this work.

**Abstract:** The distinct clinical and radiological characteristics of right temporal variant FTD have only been recently recognized. **Methods:** Eight patients with right temporal variant FTD were prospectively recruited and underwent a standardised neuropsychological assessment, clinical MRI, and quantitative neuroimaging. **Results:** Our voxelwise grey analyses captured bilateral anterior and mesial temporal grey matter atrophy with a clear right-sided predominance. Bilateral hippocampal involvement was also observed, as well as disease burden in the right insular and opercula regions. White matter integrity alterations were also bilateral in anterior temporal and sub-insular regions with a clear right-hemispheric predominance. Extra-temporal white matter alterations have also been observed in orbitofrontal and parietal regions. Significant bilateral but right-predominant thalamus, putamen, hippocampus, and amygdala atrophy was identified based on subcortical segmentation. The clinical profile of our patients was dominated by progressive indifference, decline in motivation, loss of interest in previously cherished activities, incremental social withdrawal, difficulty recognising people, progressive language deficits, increasingly rigid routines, and repetitive behaviours. **Conclusions:** Right temporal variant FTD has an insidious onset and may be mistaken for depression at symptom onset. It manifests in a combination of apathy, language, and behavioural features. Quantitative MR imaging captures a characteristic bilateral but right-predominant temporal imaging signature with extra-temporal frontal and parietal involvement.

**Keywords:** ALS; FTD; MRI; biomarker; sbvFTD; neuroimaging; cognition; neuropsychology



**Citation:** Kleinerova, J.; McKenna, M.C.; Finnegan, M.; Tacheva, A.; Garcia-Gallardo, A.; Mohammed, R.; Tan, E.L.; Christidi, F.; Hardiman, O.; Hutchinson, S.; et al. Clinical, Cortical, Subcortical, and White Matter Features of Right Temporal Variant FTD. *Brain Sci.* **2024**, *14*, 806. <https://doi.org/10.3390/brainsci14080806>

Academic Editor: Juan Francisco Vázquez-Costa

Received: 20 July 2024

Revised: 5 August 2024

Accepted: 9 August 2024

Published: 11 August 2024



**Copyright:** © 2024 by the authors. Licensee MDPI, Basel, Switzerland. This article is an open access article distributed under the terms and conditions of the Creative Commons Attribution (CC BY) license (<https://creativecommons.org/licenses/by/4.0/>).

## 1. Introduction

Frontotemporal dementia (FTD) encompasses a wide spectrum of neurodegenerative disorders that may be further stratified according to clinical phenotype, genotype, or the underlying molecular pathology [1–6]. The striking clinical, radiological, genetic, and molecular heterogeneity of FTD is well recognised and clinical subtypes are defined based on unique clinical and radiological features [3,7]. On clinical grounds, language-variant and behavioural-variant phenotypes are typically distinguished first before subcategorising patients into specific categories based on detailed neuropsychological data. The overlap with Amyotrophic Lateral Sclerosis is also well recognised with a number of shared radiological and pathological features [8–13]. Individuals harbouring hexanucleotide GGGCC repeat expansions in *C9orf72*, in particular, are at risk of developing either ALS, FTD, or ALS-FTD [14,15]. ALS-FTD as a distinct entity has been recognised before the discovery of *C9orf72* repeat expansions and has been extensively studied through robust neuropsychology, post mortem, and neuroimaging studies [16–18].

Semantic variant primary progressive aphasia (svPPA) is an FTD phenotype that clinically manifests as anomia and impaired single-word comprehension [1,19], is radiologically

defined by dominant-hemispheric anterior temporal lobe atrophy [1], and is pathologically characterised by frontotemporal lobar degeneration transactive response DNA-binding protein 43 (FTLD-TDP-43) pathology type C in the majority of cases [20]. In recent times, it has become apparent that non-dominant anterior temporal lobe atrophy presents with a distinct clinical phenotype that initially does not meet the classification criteria for svPPA [1,21]. A vast range of alternative terminology has been used to describe this entity: ‘right temporal variant FTD’, ‘right temporal semantic dementia’, ‘right temporal svPPA’, and ‘right temporal behavioural variant FTD (bvFTD)’. Clinical algorithms have been proposed to differentiate this presentation from other FTD phenotypes and other neurodegenerative disorders [22]. A recent study outlined the longitudinal clinical characteristics of this cohort, proposing dedicated classification criteria with streamlined nomenclature highlighting the main symptomatology: ‘semantic behavioural variant FTD’ (sbvFTD) [23].

The proposed classification criteria for sbvFTD require at least two core criteria: loss of empathy; difficulty identifying and naming people; rigid thought processes or complex compulsions; and at least 2 supportive criteria: object-naming difficulties, spared visuospatial functions, and spared motor speech and phonology [23]. It may be a particularly difficult diagnosis early in the course of the disease and often mistaken for psychiatric illnesses [23]. The behavioural and language manifestations later progress and overlap with other FTD phenotypes, particularly svPPA and bvFTD [24–27]. It is radiologically defined by non-dominant anterior temporal lobe atrophy with progressive bilateral orbitofrontal cortex, anterior cingulate, and contralateral anterior temporal lobe atrophy [24]. FTLD TDP-43 type C is the most commonly reported pathology [21,23,25]. While sbvFTD is increasingly recognised as a distinct phenotype, relatively few case series have been published, and it is a particularly challenging diagnosis to establish as atrophy patterns can be challenging to appreciate on standard clinical imaging. Accordingly, our objective is the detailed clinical and radiological profiling of a cohort of patients with sbvFTD using standardised clinical instruments and a standardised quantitative neuroimaging protocol.

## 2. Materials and Methods

### Ethics Approval

All aspects of this project were approved by the Ethics Committee of Beaumont Hospital Dublin (REC reference: 08/90), and each participant gave informed consent prior to study enrolment.

### Participants

A total of 8 participants with right temporal variant FTD and 100 healthy controls were included in this study. All patients first had standard clinical T1-weighted, FLAIR and DWI MRI imaging, and 4 patients also underwent [<sup>18</sup>F] FDG PET-CT imaging. A total of 7 patients and 100 healthy controls (Table 1) additionally underwent high-resolution 3D T1-weighted imaging to map patterns of grey matter atrophy and diffusion tensor imaging for quantitative white matter analyses using the same scanner and a standardised neuroimaging protocol described below. Seven patients had a standardised neuropsychological evaluation with the Edinburgh Cognitive and Behavioural ALS Screen (ECAS) [28]. Three patients had comorbid Amyotrophic Lateral Sclerosis, fulfilling the El Escorial criteria [29]. Exclusion criteria for both patients and controls included prior cerebrovascular events (strokes), prior neurosurgery, traumatic brain injury, malignancies, demyelination, and paraneoplastic syndromes. None of the healthy controls had a family history of dementia, psychiatric diagnoses, or motor neuron disease among their first- and second-degree relatives.

**Table 1.** The demographic profile of patients with semantic behavioural variant FTD (sbvFTD) and healthy controls (HC) who underwent quantitative grey and white matter neuroimaging.

	Semantic–Behavioural Variant FTD (sbvFTD) n = 7	Healthy Controls (n = 100)	Group Comparisons
Age (Years—M/SD)	67.29 (4.92)	65.23 (6.52)	0.416
Sex (M/F)	4/3	56/44	0.953
Education (Years—M/SD)	14.43 (3.99)	14.92 (3.34)	0.711
Handedness (Rt/Lt)	6/1	88/12	0.858
Symptom duration (Years—M/SD)	5.86 (2.41)	n/a	n/a

Notes. Group-differences in age and education were examined with one-way analysis of variance and differences in sex and handedness distributions between patients with semantic-behavioural variant and healthy controls were contrasted with chi-square test ( $\chi^2$ ) tests. Abbreviations: HC—healthy controls, Lt—left, M—mean, Rt—right, sbvFTD—semantic-behavioural variant FTD, SD—standard deviation.

### Neuroimaging

Neuroimaging data were acquired with a standardised protocol on a 3 Tesla Philips Achieva MR platform. The protocol included fluid-attenuated inversion recovery (FLAIR), 3D T1-weighted (T1w), and diffusion-tensor (DWI) pulse sequences. FLAIR images were acquired axially with an Inversion Recovery Turbo Spin Echo (IR-TSE) sequence with the following settings: repetition time (TR)/echo time (TE) = 11,000/125 ms, inversion time (TI) = 2800 ms, field of view (FOV) = 230 × 183 × 150 mm, voxel resolution (VR) = 0.65 × 0.87 × 4 mm. T1w images were acquired with a 3D Inversion Recovery Prepared Spoiled Gradient Recalled Echo (IR-SPGR) sequence with the following parameters: TR/TE = 8.5/3.9 ms, TI = 1060 ms, FOV of 256 × 256 × 160 mm, 160 sagittal slices with no interslice gap, flip angle (FA) = 8°, VR = 1 mm<sup>3</sup>, SENSE factor = 1.5. Diffusion-weighted images (DWI) were obtained with a spin-echo echo planar imaging (SE-EPI) pulse sequence to acquire DWI data with a 32-direction Stejskal–Tanner diffusion encoding scheme: TR/TE = 7639/59 ms, FOV = 245 × 245 × 150 mm, 60 axial slices with no interslice gaps, FA = 90°, VR = 2.5 mm<sup>3</sup>, SENSE factor = 2.5, dynamic stabilisation and spectral presaturation with inversion recovery (SPIR) fat suppression.

### Morphometric analyses

Patterns of grey matter atrophy in the semantic behavioural variant frontotemporal dementia cohort were evaluated by voxel-based morphometry (VBM) in contrast to the cohort of the age- and sex-matched healthy controls. FMRIB’s FSL suite was utilised to conduct the VBM analyses. [30–32] Standard pre-processing pipelines were implemented with skull-removal (BET) [33], motion-correction, and tissue-type segmentation. Subsequently, grey matter partial volume images were aligned to the MNI152 standard space using affine registration. A study-specific GM template was created thereafter to which the grey matter images from each subject were non-linearly co-registered. Permutation-based non-parametric inference [34] was used for group comparisons, controlling for total intracranial volumes (TIV), sex, age, and education. TIV was calculated by linearly aligning each participant’s brain image to the MNI152 standard, and the inverse of the determinant of the affine registration matrix was calculated and multiplied by the size of the template. The threshold-free cluster enhancement (TFCE) method [35] was implemented to correct for multiple comparisons. Resulting statistical maps were visualised in FSLEYES and thresholded at  $p < 0.01$  to characterise focal grey matter vulnerability patterns.

### White matter analyses

Pre-processing of the raw diffusion data included eddy current corrections and skull removal before a tensor model was fitted to the data to generate maps of axial diffusivity (AD), fractional anisotropy (FA), radial diffusivity (RD), and mean diffusivity (MD). The tract-based statistics (TBSS) stream [36] of FMRIB's FSL image analysis suite was implemented for non-linear registration and skeletonisation of each subject's images. FA, AD, MD, and RD images were merged into a single 4D image file, and a mean FA mask was created. Permutation-based non-parametric inference was used for the voxelwise comparison of diffusivity parameters between patients with semantic behavioural variant frontotemporal dementia and healthy controls using design matrix-defined contrasts incorporating age, sex, and education as covariates. The threshold-free cluster enhancement (TFCE) method was implemented, and resulting statistical maps were thresholded at  $p < 0.0125$  TFCE family-wise error (FWE).

### Subcortical segmentation

The standard anatomical segmentation pipeline of the FreeSurfer image analysis suite [37] was first implemented with 'recon-all', which includes non-parametric non-uniform intensity normalisation, affine registration to the MNI305 atlas, intensity normalisation, skull stripping, automatic subcortical segmentation, linear volumetric registration, neck removal, tessellation of the grey matter–white matter boundary, surface smoothing, inflation to minimise metric distortion, and automated topology correction [38]. The automated subcortical segmentation pipeline of FreeSurfer relies on a probabilistic atlas [39]. Segmentation accuracy has been individually reviewed for all subjects. Estimated total intracranial volumes (eTIV) were calculated in FreeSurfer using Buckner's approach [40] and subsequently used as a covariate in group comparisons in addition to age, sex, and education.

### Data availability

Clinical, genetic, or neuroimaging data from individual patients cannot be made available due to departmental policies, but additional information on data-processing pipelines can be requested from the corresponding author.

### Statistics

Group differences in age and education were examined with one-way analysis of variance, and differences in sex and handedness distributions between patients with semantic–behavioural variants and healthy controls were contrasted with chi-square ( $\chi^2$ ) tests (Table 1). As described above, non-parametric permutation-based testing was utilised for voxelwise grey and white matter analyses. The design matrices included age, sex, and education as covariates and total intracranial volumes (eTIV) were included as additional covariates as for voxel-based morphometry. The resulting statistical maps were corrected for family-wise error. No statistical analyses were run on PET data.

To test the effect of group on subcortical volumes, a multivariate analysis of covariance (MANCOVA) was conducted with the volumes of individual structures as dependent variables, the study group (HC, sbvFTD) as independent factor and age, sex, education, and eTIV as covariates. In case of a significant multivariate omnibus test, post hoc univariate comparisons were considered significant at  $p < 0.05$ , following Bonferroni corrections for multiple comparisons to reduce Type I error. These analyses were conducted using IBM SPSS v. 29.

## **3. Results**

### *3.1. Grey Matter Atrophy Patterns*

The demographic profiles of those included in quantitative neuroimaging analyses are summarised in Table 1. Voxel-based morphometry revealed bilateral anterior and mesial temporal atrophy with right-sided predominance. Patterns of atrophy also affected the bilateral hippocampi and the right insular and opercula region (Figure 1).

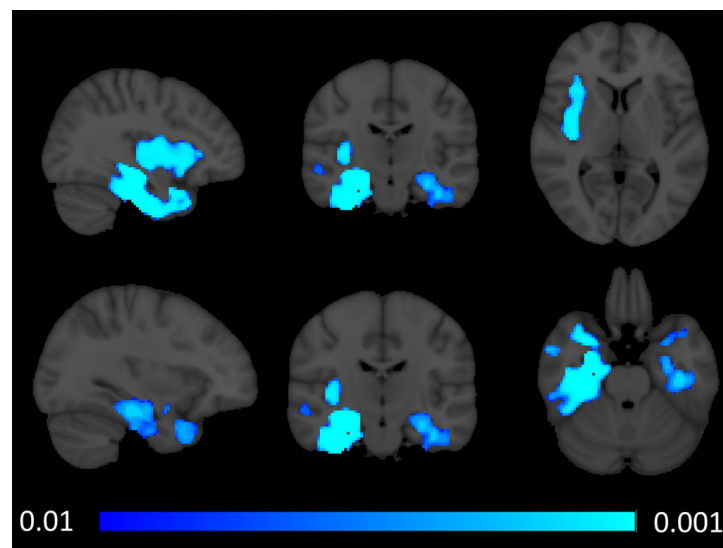


**Figure 1.** Patterns of cortical grey matter signal reduction in sbvFTD based on voxel-based morphometry outputs at  $p$  FWE TFCE  $< 0.01$  corrected for age, sex, total intracranial volume, and education. MNI coordinates (x, y, z)—top row: 36, -17, 5, bottom row: -32, -17, and -26.

### 3.2. White Matter Patterns

Tract-based spatial statistics captured increased axial diffusivity (AD) in the right anterior temporal lobe in patients with semantic behavioural variant frontotemporal dementia (Figure 2). Similar to the voxel-based morphometry results, fractional anisotropy (FA) reductions were noted bilaterally in both anterior temporal and sub-insular regions with a marked predominance to the right hemisphere (Figure 3). In addition to the temporal and insular white matter integrity changes, right-predominant orbitofrontal and parietal FA alterations were also noted at  $p < 0.0125$  FEW-corrected. Increased radial diffusivity was noted in the right temporal lobe with a clear anterior predominance (Figure 4), but also some orbitofrontal and sub-insular involvement. Mean diffusivity increases were confined to the right anterior temporal lobe and right insular regions (Figure 5).

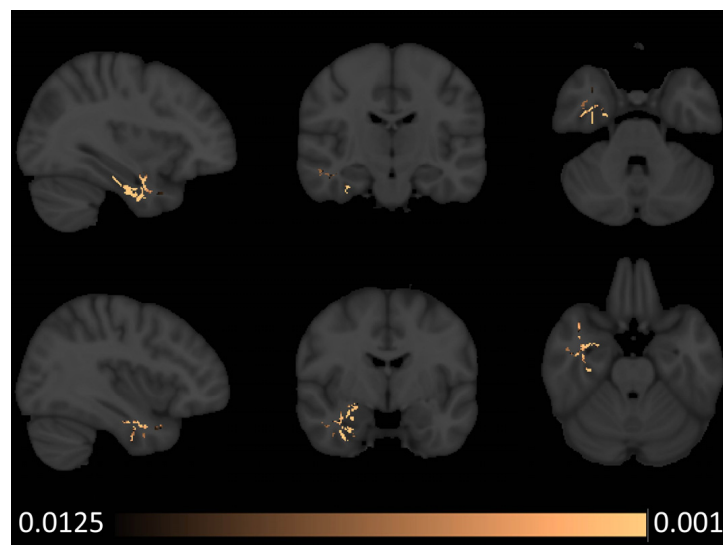


**Figure 2.** Patterns of axial diffusivity (AD) alterations in sbvFTD based on tract-based statistics outputs thresholded at  $p$  FWE TFCE  $< 0.0125$  corrected for age, sex, and education. MNI coordinates (x, y, z)—top row: 34, -17, and -33; bottom row: 38, -5, and -25.

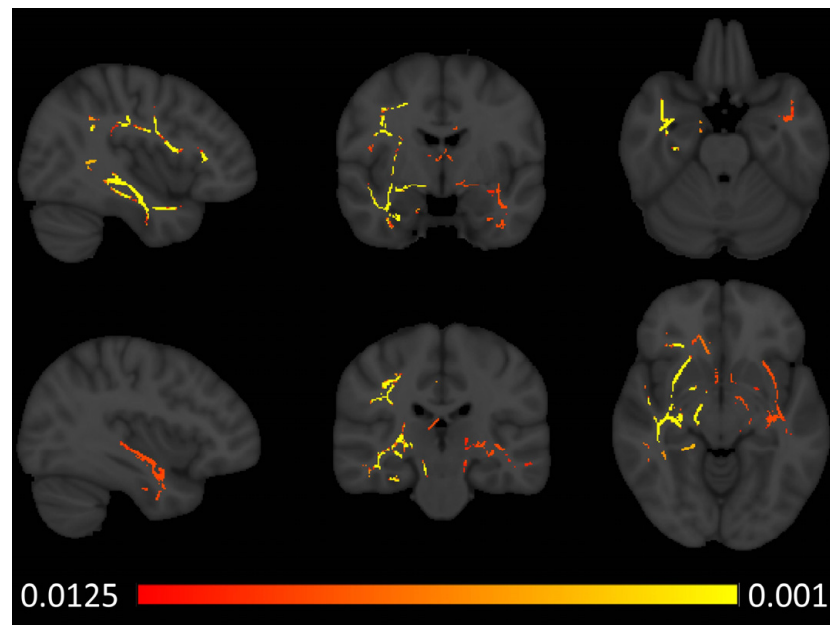


**Figure 3.** Patterns of fractional anisotropy (FA) reductions in sbvFTD based on tract-based statistics outputs thresholded at  $p$  FWE TFCE  $< 0.0125$  corrected for age, sex, and education. MNI coordinates (x, y, z)—top row: 41, -5, and -24, bottom row: -36, -23, and -7.

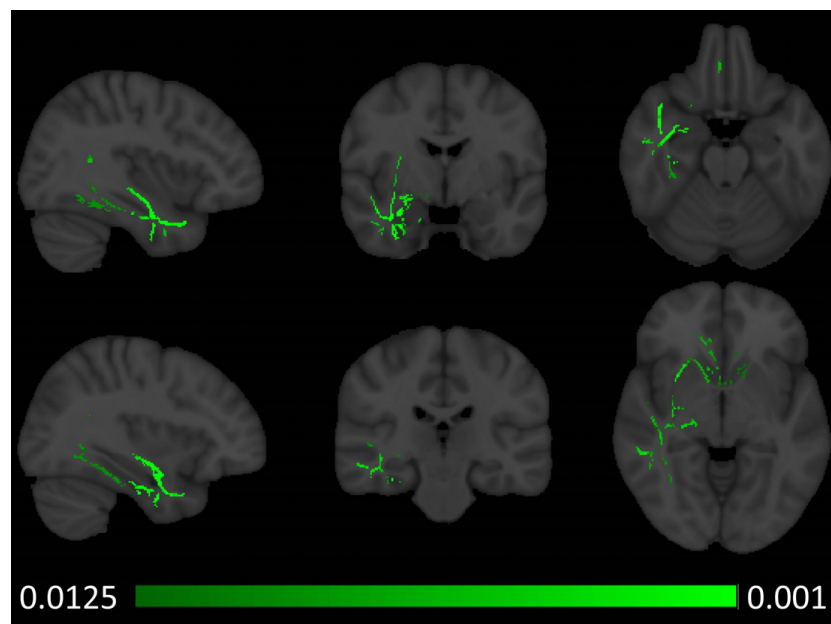


**Figure 4.** Patterns of radial diffusivity (RD) alterations in sbvFTD based on tract-based statistics outputs thresholded at  $p$  FWE TFCE  $< 0.0125$  corrected for age, sex, and education. MNI coordinates (x, y, z)—top row: 37, -3, and -22, bottom row: 34, -25, and -4.

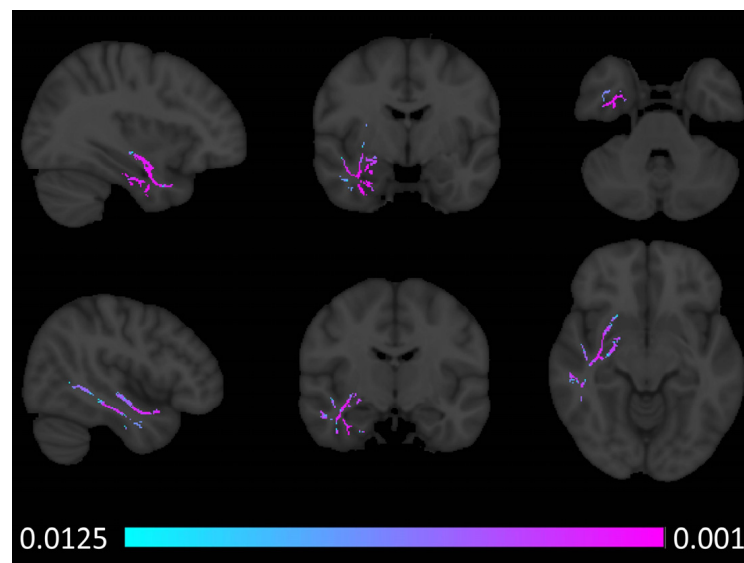


**Figure 5.** Patterns of mean diffusivity (MD) alterations in sbvFTD based on tract-based statistics outputs thresholded at  $p$  FWE TFCE  $< 0.0125$  corrected for age, sex, and education. MNI coordinates (x, y, z)—top row: 34, -5, and -35, bottom row: 45, -10, and -10.

### 3.3. Concordance with PET

Four patients had additional PET imaging, which revealed a relative concordance between focal PET hypometabolism and volume loss based on visual inspection (Figure 6).

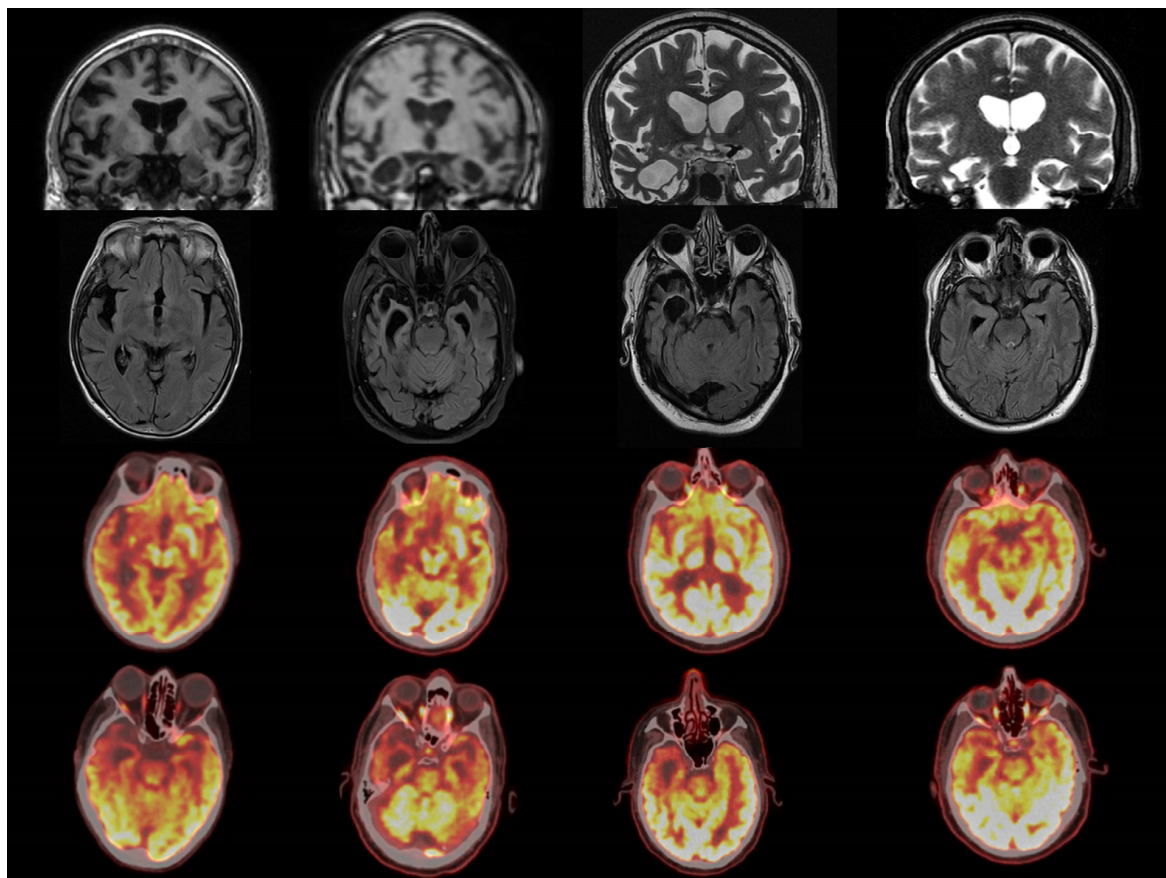


**Figure 6.** Concordance of structural changes on clinical MRIs and metabolic patterns on [ $^{18}\text{F}$ ] FDG PET-CT.

### 3.4. Subcortical Grey Matter Volume Alterations

There was a significant group effect on subcortical grey matter volumes (Pillai's Trace = 0.684,  $F(14,88) = 13.608$ ,  $p < 0.001$ ,  $\eta^2p = 0.684$ ). Significant differences were detected in the volumes of most subcortical structures between patients with sbvFTD and controls after Bonferroni corrections for multiple comparisons: left thalamus ( $p < 0.001$ ), left caudate ( $p = 0.014$ ), left putamen ( $p < 0.001$ ), left pallidum ( $p < 0.001$ ), left hippocampus ( $p < 0.001$ ), left amygdala ( $p < 0.001$ ), right thalamus ( $p < 0.001$ ), right caudate ( $p < 0.001$ ), right putamen ( $p < 0.001$ ), right hippocampus ( $p < 0.001$ ), right amygdala ( $p < 0.001$ ), and right accumbens area ( $p < 0.001$ ). Based on  $\eta^2p$  values, larger effect sizes were identified for most right hemispheric structures compared to the left ones. The volumetric profile of the two study groups is summarised in Table 2, reporting estimated marginal means and standard error in patients with sbvFTD and healthy controls, as well as univariate effect sizes and corrected  $p$ -values (Table 2).

**Table 2.** Subcortical grey matter volumetric profiles in sbvFTD and healthy controls (HC).

Subcortical Structure	Estimated Marginal Means $\pm$ S.E.		Statistics	
	HC (n = 100)	sbvFTD (n = 7)	Univariate Effect Size	$p$ -Corrected
Thalamus L	7360.36 $\pm$ 81.57	5687.58 $\pm$ 314.29	$\eta^2p = 0.207$	<b>&lt;0.001</b>
Thalamus R	6916.73 $\pm$ 64.76	5180.82 $\pm$ 249.52	$\eta^2p = 0.309$	<b>&lt;0.001</b>
Caudate L	3426.86 $\pm$ 36.60	2945.77 $\pm$ 141.01	$\eta^2p = 0.097$	<b>0.014</b>
Caudate R	3526.19 $\pm$ 36.89	2575.97 $\pm$ 142.12	$\eta^2p = 0.292$	<b>&lt;0.001</b>
Putamen L	4638.97 $\pm$ 48.63	3641.45 $\pm$ 187.39	$\eta^2p = 0.207$	<b>&lt;0.001</b>
Putamen R	4672.54 $\pm$ 49.51	2943.83 $\pm$ 190.77	$\eta^2p = 0.431$	<b>&lt;0.001</b>
Pallidum L	1940.44 $\pm$ 20.36	1599.42 $\pm$ 78.44	$\eta^2p = 0.148$	<b>&lt;0.001</b>
Pallidum R	1894.54 $\pm$ 25.57	1805.70 $\pm$ 98.50	$\eta^2p = 0.007$	1.000
Hippocampus L	4064.14 $\pm$ 42.90	3334.91 $\pm$ 165.30	$\eta^2p = 0.152$	<b>&lt;0.001</b>
Hippocampus R	4199.83 $\pm$ 42.64	2650.79 $\pm$ 164.28	$\eta^2p = 0.451$	<b>&lt;0.001</b>
Amygdala L	1594.03 $\pm$ 20.70	1166.33 $\pm$ 79.77	$\eta^2p = 0.210$	<b>&lt;0.001</b>
Amygdala R	1833.13 $\pm$ 21.22	1047.12 $\pm$ 81.76	$\eta^2p = 0.460$	<b>&lt;0.001</b>
Accumbens area L	442.79 $\pm$ 9.33	338.15 $\pm$ 35.95	$\eta^2p = 0.072$	0.084
Accumbens area R	528.35 $\pm$ 8.56	271.90 $\pm$ 32.96	$\eta^2p = 0.358$	<b>&lt;0.001</b>

Notes. Estimated marginal means  $\pm$  S.E. for volumes of subcortical structures are adjusted for age, sex, education, and TIV. Post hoc univariate comparisons between groups were performed following a significant multivariate omnibus test: Pillai's Trace = 0.684,  $F(14,88) = 13.608$ ,  $p < 0.001$ ,  $\eta^2p = 0.684$ . Bold  $p$ -values are significant at  $p < 0.05$  following Bonferroni corrections for multiple comparisons. Partial  $\eta^2$  effect size is interpreted as small ( $\eta^2p = 0.01$ ), medium ( $\eta^2p = 0.06$ ), or large ( $\eta^2p = 0.14$ ).

### 3.5. Clinical Profiles

Six patients had a detailed clinical assessment with neuropsychological screening. The main findings are summarised in Table 3.



**Table 3.** The clinical profile of eight representative cases with semantic behavioural-variant FTD (sbvFTD).

	Case 1	Case 2	Case 3	Case 4	Case 5	Case 6	Case 7	Case 8
<b>Handedness</b>	Rt	Rt	Rt	Rt	Rt	Lt	Rt	Rt
<b>Age</b>	73	65	71	67	73	64	61	64
<b>Sex</b>	M	M	F	M	F	M	M	F
<b>Education (years)</b>	17	17	10	15	20	9	13	15
<b>Symptom Duration</b>	2 years	8 years	3 years	10 years	8 years	7 years	6 years	7 years
<b>Presenting symptoms</b>								
Prosopagnosia	✓	✓	✓	✓	✓	✓	✓	-
Rigid thought process	✓	-	✓	✓	✓	✓	✓	✓
Executive deficits	✓	✓	✓	✓	✓	✓	✓	✓
Obs. Rep. behaviours	✓	-	✓	✓	✓	-	✓	-
Verbal semantic loss	-	✓	-	✓	✓	✓	✓	✓
Ep. Mem. impairment	-	✓	✓	✓	✓	✓	-	-
Disinhibition	✓	-	-	✓	✓	-	✓	✓
Loss of empathy	✓	✓	✓	-	-	✓	-	-
Apathy	✓	-	✓	-	-	✓	✓	✓
Dietary changes	✓	-	-	-	-	-	-	✓
Alexithymia	✓	✓	-	✓	-	-	✓	-
<b>Comorbid dx.</b>	-	Hypertension	ALS	-	-	-	ALS	ALS
<b>ACE-III</b>	97/100	89/100	63/100	41/100	91/100	88/100	61/100	93/100
<b>ECAS</b>	120/136	95/136	85/136		109/136	92/136	81/136	112/136
<b>BNT</b>	25/30	24/30	21/30	-	14/30	21/30	17/30	19/30
	Executive Language Memory - Attention	Executive Language Memory Fluency -	Executive Language Memory -	Executive Language Memory Fluency -	Executive Language Memory Fluency -	Executive Language Memory Fluency Attention	Executive Language Memory Fluency -	Executive Language Memory Fluency -
<b>CSF</b>	Not AD-compatible	-	-	-	Not AD-compatible	Not AD-compatible	-	-
<b>AB42 (591–997 pg/mL)</b>	835	-	-	-	959.6	722.2	-	-
<b>Total Tau (135–345 pg/mL)</b>	602.7	-	-	-	249	302	-	-
<b>P-Tau (35.0–64.0 pg/mL)</b>	116.5	-	-	-	46	67.3	-	-
<b>Neuroimaging</b>								
Clinical MRI	✓	✓	✓	✓	✓	✓	✓	✓
[18F] FDG PET-CT	✓	-	-	✓	✓	✓	-	-
Quantitative 3D MRI	✓	✓	✓	-	✓	✓	✓	✓

**Notes:** ACE—The Addenbrooke’s Cognitive Examination, BNT—The Boston Naming Test, CSF—cerebrospinal fluid, Dx.—diagnosis, ECAS—Edinburgh Cognitive and Behavioural ALS Screen, Ep. Mem. impairment—episodic memory impairment, FDG PET-CT—fluorodeoxyglucose positron emission tomography, Lt—left, M—mean, Obs. Rep. behaviour—obsessive repetitive behaviours, Rt—right.

#### 4. Discussion

This study highlights the core and radiological features of sbvFTD. The systematic assessment of a cohort of patients with sbvFTD in a single-centre setting and the computational analyses of MRI data acquired with a standardised radiological protocol allow the description of unifying anatomical features.

##### Clinical observations

Despite differences in symptom duration, our cohort exhibited relatively unifying clinical features. All cases had initial insight into their deficits. All cases presented with rigid thought processes, executive dysfunction, and varying degrees of prosopagnosia; the majority had verbal semantic loss, obsessive repetitive behaviours, and episodic memory impairment; and some also had a loss of empathy, apathy, disinhibition, alexithymia, and

dietary changes. The main cognitive domains affected were executive, language, fluency, and memory. Most cases had anomia with varying levels of impaired comprehension. Surface dyslexia was also observed. All of the patients exhibited progressive indifference and a decline in motivation. The initial indifference and lack of motivation in 3 out of 8 cases were initially mistaken for depression. A loss of interest in previously cherished activities, such as reading, playing golf, and gardening, was a common theme. Incremental social withdrawal was invariably reported, which is likely to be multifactorial in the majority of cases due to loss of interest in friends and relatives, difficulty recognising people, and language deficits. Many of our patients developed an increasingly rigid routine, such as repetitively watching the same movie, going for long drives to the same location, listening to the same music, and taking the train to a specific destination to get an ice cream every day. In addition to the development of a regimented routine, increasingly rigid and obsessive behaviours were exhibited by some, such as only charging their mobile phone to exactly 100%. Difficulty recognising people, including familiar faces, is a common complaint in this cohort, and one patient explained that she mostly identifies people by their voices. Relentlessly evolving language deficits have particularly severe quality of life ramifications, impacting employment, job fulfilment, and enjoyment of social interactions. Increasing difficulty with both low- and high-frequency objects, variable levels of semantic deficits, frequent circumlocution, and perseveration increasingly affect both professional communication at work and informal communication in the community. Even with relatively preserved verbal fluency, digression into tangential anecdotes was noted in three patients. Family members of affected patients reported notable changes in the character of their loved ones. Three patients developed a preference for sweet foods, a symptom commonly observed in both FTD phenotypes and ALS [41]. One patient described a marked change in musical taste at the onset of symptoms, which the family found unusual. Inappropriate comments, reference to a passive death wish, and perseverative thoughts ruminating on previous work issues have also been observed in our cohort. A relative lack of empathy was noted in two patients when their partner became tearful during the consultation. Increasing difficulty using everyday technology, such as mobile phones and laptops, is also commonly reported. One patient became a victim of online fraud due to impaired judgment.

#### Radiological considerations

Our voxelwise grey analyses captured bilateral anterior and mesial temporal grey matter atrophy with a clear right-sided predominance. Bilateral hippocampal involvement was also observed, as well as disease burden in the right insular and opercula region (Figure 1). Similar to the bilateral grey matter patterns, bilateral white matter integrity alterations were noted bilaterally in anterior temporal and sub-insular regions with a clear right-hemispheric predominance. Interestingly, extra-temporal white matter alterations have also been observed in orbitofrontal (FA and RD) and parietal (FA) regions. The sensitivity profiles of the various diffusivity metrics to capture sbvFTD-associated changes differed significantly. While both FA and RD detected bilateral temporal and extra-temporal changes in orbitofrontal regions, parietal change was only detected by FA, and MD only detected right anterior temporal lobe and right insular white matter changes. FA is the most widely used diffusivity metric, which is generally considered sensitive to focal white matter integrity alterations, albeit histopathologically relatively non-specific. Traditionally, axial diffusivity is often conceptualised as an 'axonal' measure [42], whereas RD has been classically regarded as a myelin-related marker [43], although this interpretation of diffusivity alteration is likely to be simplistic. Notwithstanding the differences between the statistical maps generated based on the different diffusivity metrics, the integrative interpretation of the voxel-based morphometry and tract-based statistics results is that sbvFTD affects the bilateral temporal lobes, and extra-temporal frontal and parietal changes can also be readily captured. In addition to the anatomical concordance of our grey and white matter analyses, metabolic profiles on PET imaging have also been strikingly concurring (Figure 6), highlighting bilateral but right-predominant hypometabolism with varying degrees of

extra-temporal involvement. The review of individual PET images reveals a degree of heterogeneity in the anatomical extent and symmetry of neurodegeneration. While some patients in our cohort exhibit relatively focal right temporal-predominant degeneration, others exhibit more widespread changes. Furthermore, while all patients had a standard clinical MRI before enrolling in this imaging study, the visual review of their original clinical T1-weighted clinical images did not permit the detection of extra-temporal atrophy. The review of their initial clinical DWI/ADC and FLAIR images was unsuitable for the detection of the underlying white matter degeneration. This highlights the importance of acquiring high-resolution 3D T1w images in the clinical setting, as these permit quantitative post hoc analyses, as demonstrated in this study. We would also advocate the inclusion of a short DTI protocol so that underlying white matter integrity changes can be mapped computationally.

#### Academic considerations

The clinical and radiological profiles of our cohort are largely consistent with the existing sbvFTD literature. The average age of symptom onset is typically in the early 60s [23]. It often affects highly educated individuals [23] and presents with predominantly behavioural symptoms initially, such as loss of empathy, rigid thought processes, and loss of person-specific knowledge [23,27]. It has been proposed that the terminology ‘loss of person-specific semantic knowledge’ better encapsulates the multi-modal loss of person-specific concepts—face, voice, name, or biographical information—rather than ‘prosopagnosia’, which merely refers to difficulty recognising faces [21,23]. This deficit tends to precede the loss of verbal semantic knowledge which corresponds with the anatomical progression of the disease to the contralateral anterior temporal lobe. In addition to the ‘loss of person-specific semantic knowledge’ [22], there are some early clinical features that help to distinguish sbvFTD from other FTD phenotypes, despite the considerable clinical overlap that ensues later [22–24]. In contrast to svPPA [1], sbvFTD presents with early behavioural rather than language impairment [25]. Compulsive behaviours tend to be driven by verbal targets (e.g., fixation on charging a phone to 100%) rather than visual targets (e.g., cleaning dishes) [25]. These behaviours include ritualistic preoccupations [22], such as getting an ice cream at the same place every day. In contrast to bvFTD [6,44], insight is initially preserved [27], episodic memory is often impaired [22,27], language dysfunction is more marked [45], dietary changes are less frequent [22], and disinhibition tends to be more subtle in sbvFTD [23]. The lateralisation of language may also influence the clinical phenotype. Most people are left-hemispheric dominant, irrespective of their handedness [46]. Indeed, in the largest case series of sbvFTD, 15% of cases were left-handed or ambidextrous [23]. From a radiological perspective, sbvFTD is classically associated with subdominant temporal lobe atrophy and hypometabolism [47]. There is progressive medial-to-lateral gradient anterior temporal lobe [22,27,48] atrophy associated with ipsilateral insular [22], hippocampal [27,48], amygdalar [25,27,48,49], and fusiform gyrus [22,48] atrophy. Subdominant temporal lobe atrophy correlates with a loss of socioemotional non-verbal semantic knowledge [23], e.g., recognising emotion [45,49–53], peoples’ faces [22,24], and social cues [53,54]. Focal hypometabolism correlates with psychiatric symptoms, low mood, and anxiety [55]. The disease later progresses to involve the contralateral anterior temporal lobe [22,23,25,27,48], hippocampus [27,48], amygdala [27,48], fusiform gyrus [48], bilateral anterior cingulate [24], and orbitofrontal regions [21,22,24,25,49] [22]. The degree of atrophy inversely correlates with disease duration [25]. Similar to svPPA, FTLT-DTP43 type C is the most commonly reported pathology [21,56]; however, FTLT-tau and FTLT-DTP43 type A and B have also been described [56,57]. The different molecular pathologies manifest in relatively different clinical phenotypes: FTLT-DTP43 type C leads to a temporal predominant degeneration associated with prominent semantic impairment, whereas FTLT-tau and FTLT-DTP43 types A and B lead to frontal-predominant degeneration with prominent behavioural impairment [56,57].

## ALS-FTD

While sbvFTD is a well-recognised clinical entity, ALS-associated sbvFTD is not typically considered as a separate phenotype. ALS-FTD has an ever-growing literature [58,59]. After a series of early descriptions of ALS cases with marked behavioural impairment [60], the identification of GGGGCC hexanucleotide repeat expansions in ALS has given considerable impetus to ALS-FTD research [61]. Imaging studies in ALS have gradually shifted their focus from primary motor regions to the evaluation of frontotemporal, cerebellar, and subcortical regions [18,59,62–68]. While initially, executive dysfunction, verbal fluency deficits, pseudobulbar affect, and disinhibition were considered the hallmarks of ALS-associated neuropsychological profile [12,16,60,69,70], the high incidence of comorbid language deficits, memory impairment, apathy, and deficits in social cognition were also increasingly recognised in ALS [71–78]. The practical ramifications of cognitive and behavioural impairment in ALS cannot be underestimated [79], as they impact survival, compliance with assistive devices, participation in clinical trials, and caregiver burden [80,81]. Language deficits in ALS have been previously linked to both grey and white matter degeneration [73], apathy has been linked to nucleus accumbens atrophy [82], memory impairment to hippocampal pathology [83], and amygdala [84,85] and thalamus degeneration has been implicated in multi-domain deficits [86,87], but sbvFTD is not universally recognised as a separate entity in ALS.

## Subcortical involvement in ALS-FTD and FTD phenotypes

The physiology role of specific subcortical nuclei in relaying distinct cortico-cortical and cortico-basal networks is well described [88,89], and these networks have been implicated in disease propagation in ALS and ALS-FTD [90,91]. Thalamic degeneration is particularly well characterised across the spectrum of ALS-FTD phenotypes [86,92–95]. Subcortical involvement and frontotemporal dysfunction are also recognised in less common motor neuron disease phenotypes, such as primary lateral sclerosis [96,97]. Presymptomatic thalamic changes have been described in GGGGCC hexanucleotide repeat expansion carriers by several groups long before projected symptom onset [98–100]. However, hexanucleotide repeat expansion status is not the sole determinant for subcortical degeneration in ALS; considerable thalamic and subcortical grey matter degeneration can also be observed in *C9orf72* negative ALS cohorts [101,102]. Hippocampal degeneration also has considerable literature in both FTD [103] and ALS [83,104], and more recent studies have examined specific hippocampal subfields separately as they relay different networks and contribute to the function of specific limb circuits including Papez circuit [105–107]. Accumbens nucleus and amygdalar degeneration [84] are also well recognised along the ALS-FTD spectrum and have been linked to specific neurocognitive manifestations [108], but differences in left and right hemispheric pathology are seldom specifically evaluated. While the cortical profile of sbvFTD is well characterised [47,56], subcortical involvement is less well studied.

## Clinical implications

As demonstrated by the clinical profile of our cohort, right temporal variant ALS-FTD/FTD may be initially mistaken for depression or psychiatric conditions, and there may be a very significant interval between symptom onset and definite diagnosis. Misdiagnoses and diagnostic delays not only cause frustration in affected families but also delay supportive interventions, genetic screening, timely resource allocation, capacity testing, etc. The wider recognition of sbvFTD will eventually lead to an earlier diagnosis of these patients, a better understanding of disease mechanisms [23], and, ultimately, the development of robust research frameworks to accurately stratify FTD phenotypes [21]. Our report also highlights the role of PET imaging in suspected cases and the limitations of visual inspection of standard clinical MRI. While in advanced disease, visual inspection of structural images may reveal ex vacuo ventricular dilation and widened sulci, these images are not suitable to appraise cortical thickness and density reductions, and visual inspection also precludes the assessment of deep subcortical grey matter volume reductions. Similarly, while FLAIR or T2w imaging would capture microvascular disease burden, degenerative changes in specific

white matter tracts can only be evaluated by 3D DTI-derived or more advanced (NODDI, HARDI) white matter imaging techniques [109,110]. While until recently, quantitative neuroimaging has primarily offered group-level imaging signatures in various ALS-FTD phenotypes, with the advent of novel machine-learning [111–116] and robust z-score-based approaches [117–120], single MRI data sets can now be meaningfully interpreted [121].

#### Study limitations

This study is not without limitations. Despite the relative clinical and radiological homogeneity of our cohort, there were considerable differences in the symptom duration profile of our patients. A key limitation of this study stems from its cross-sectional design. While we capture and describe a unifying radiological signature, the cross-sectional analyses preclude the characterisation of the clinical and radiological evolution of disease trajectories. Only a prospective, longitudinal, multi-time point study would elucidate anatomical propagation patterns and confirm whether progressive contralateral temporal lobe atrophy ensues eventually. Finally, we do not have accompanying neuropathology data on this cohort to offer histological descriptions and TDP-43 subtyping. Owing to the small sample size of our cohort, the imaging profile of the sbvFTD group has not been systematically contrasted to other ALS-FTD phenotypes.

#### Future directions

Large longitudinal studies are needed with a comprehensive neuropsychological battery to assess the clinical and radiological trajectory of this entity with subsequent post mortem examination and TDP-43 subtyping. In light of the heterogeneity of temporal lobe pathology in other neurodegenerative disorders, the clinical correlates of right temporal lobe pathology should also be studied in other motor neuron diseases (PLS, HSP, and SBMA), Alzheimer's disease, and movement disorders [122–130]. In the assessment of patients with suspected neurodegenerative conditions, clinical MRI protocols should routinely incorporate a 3D T1-weighted sequence and a DTI sequence to enable post hoc quantitative grey and white matter analyses, which are useful for both diagnostic and monitoring purposes.

## 5. Conclusions

Our data suggest a unifying imaging signature in sbvFTD encompassing right-predominant but bilateral temporal lobe degeneration. In addition to the striking temporal disease burden, we have also demonstrated considerable subcortical grey matter pathology, as well as insular, frontal, and parietal involvement. Due to its distinguishing clinical features, the associated diagnostic challenges and singular metabolic, diffusion, and structural signature, sbvFTD should be considered a distinct clinical phenotype along the FTLD continuum. The increasing recognition of this phenotype and increased research efforts dedicated to sbvFTD may ultimately enhance the development of consensus management protocols.

**Author Contributions:** The manuscript was drafted by J.K., M.C.M., and P.B. Study conceptualisation: J.K., M.C.M., M.F., E.L.T., F.C., S.H., and P.B. Clinical assessments: M.C.M., M.F., A.G.-G., R.M., O.H., S.H., and P.B. Data processing and analyses: J.K., M.C.M., A.T., E.L.T., F.C., and P.B. The manuscript was reviewed for intellectual content by J.K., M.C.M., M.F., A.T., A.G.-G., R.M., E.L.T., F.C., S.H., and P.B. All authors have read and agreed to the published version of the manuscript.

**Funding:** This project was sponsored by the Health Research Board Ireland (JPND-Cofund-2-2019-1 & HRB EIA-2017-019). Professor Bede and the neuroradiological aspects of this project are also supported by the Irish Institute of Clinical Neuroscience (IICN), the EU Joint Programme—Neurodegenerative Disease Research (JPND), the Science Foundation Ireland (SFI SP20/SP/8953), the Andrew Lydon scholarship, and the Iris O'Brien Foundation.

**Institutional Review Board Statement:** This research project was approved by The Beaumont Ethics Medical Research Committee, Beaumont Hospital Dublin (REC reference: 08/90, date: 1 September 2019), and all participants gave informed consent to participate.

**Informed Consent Statement:** Informed consent was obtained from all subjects involved in the study.

**Data Availability Statement:** Clinical, genetic, or neuroimaging data from individual patients cannot be made available due to departmental policies. Additional information on data-processing pipelines can be requested from the corresponding author.

**Acknowledgments:** We acknowledge the generosity of all patients and controls who have participated in this research study.

**Conflicts of Interest:** The authors declare no conflicts of interest.

## Glossary

AD: Axial Diffusivity, ALS: amyotrophic lateral sclerosis, ALSod: ALS online database, ANOVA: analysis of variance (ANOVA), ASO: antisense oligonucleotide, BOLD: blood-oxygen-level-dependent (BOLD) signal, C9+: ALS patients with GGGGCC hexanucleotide repeat expansion in *C9orf72*, C9-: ALS patients without GGGGCC hexanucleotide repeat expansion in *C9orf72*, C9orf72: chromosome 9 open reading frame 72, CC: corpus callosum, CT: cortical thickness, CST: corticospinal tract, DTI: diffusion tensor imaging, DWI: diffusion-weighted imaging, EPI: echo-planar imaging, FA: fractional anisotropy, FC: functional connectivity, fMRI: functional MRI, FLAIR: fluid-attenuated inversion recovery, FOV: field of view, FSL: FMRIB's Software Library, FTD: frontotemporal dementia, FTLD: frontotemporal lobar degeneration, FWE: familywise error, GM: grey matter, HARDI: High-Angular-Resolution Diffusion Imaging, HC: healthy control, IR-SPGR: inversion recovery prepared spoiled gradient recalled echo, LH: left hemisphere, Lt: Ltft, LMN: lower motor neuron, M1: primary motor cortex, MANCOVA: multivariate analysis of covariance, ML: machine learning, MND: motor neuron disease, MNI: Montreal Neurological Institute, MNI152: Montreal Neurological Institute 152 standard space, MRI: magnetic resonance imaging, MRS: MR spectroscopy, NISALS: Neuroimaging Society in ALS, NIV: non-invasive ventilation, NODDI: neurite orientation dispersion and density imaging, PBA: pseudobulbar affect, PCR: polymerase chain reaction, PD: Parkinson's disease, PMC: primary motor cortex, QC: quality control, RH: right hemisphere, Rt: right, RD: radial diffusivity, ROI: region of interest, rs-fMRI: resting-state functional MRI, SC: structural connectivity, SD: standard deviation, SE-EPI: spin echo planar imaging, SENSE: sensitivity encoding, SPIR: spectral presaturation with inversion recovery, T: Tesla, T1w: T1-weighted imaging, TCV: total cerebellar volume, TDI: Track Density Imaging, TE: echo time, TI: inversion time, TIV: total intracranial volume, TR: repetition time, UMN: upper motor neuron, VR: voxel resolution, WM: white matter.

## References

- Gorno-Tempini, M.L.; Hillis, A.E.; Weintraub, S.; Kertesz, A.; Mendez, M.; Cappa, S.F.; Ogar, J.M.; Rohrer, J.D.; Black, S.; Boeve, B.F.; et al. Classification of primary progressive aphasia and its variants. *Neurology* **2011**, *76*, 1006–1014. [[CrossRef](#)] [[PubMed](#)]
- Strong, M.J.; Abrahams, S.; Goldstein, L.H.; Woolley, S.; McLaughlin, P.; Snowden, J.; Mioshi, E.; Roberts-South, A.; Benatar, M.; HortobaGyi, T.; et al. Amyotrophic lateral sclerosis—Frontotemporal spectrum disorder (ALS-FTSD): Revised diagnostic criteria. *Amyotroph. Lateral Scler. Front. Degener.* **2017**, *18*, 153–174. [[CrossRef](#)] [[PubMed](#)]
- Rohrer, J.D.; Lashley, T.; Schott, J.M.; Warren, J.E.; Mead, S.; Isaacs, A.M.; Beck, J.; Hardy, J.; de Silva, R.; Warrington, E.; et al. Clinical and neuroanatomical signatures of tissue pathology in frontotemporal lobar degeneration. *Brain A J. Neurol.* **2011**, *134*, 2565–2581. [[CrossRef](#)]
- Lomen-Hoerth, C. Clinical Phenomenology and Neuroimaging Correlates in ALS-FTD. *J. Mol. Neurosci.* **2011**, *45*, 656–662. [[CrossRef](#)] [[PubMed](#)]
- Strong, M.J.; Grace, G.M.; Freedman, M.; Lomen-Hoerth, C.; Woolley, S.; Goldstein, L.H.; Murphy, J.; Shoesmith, C.; Rosenfeld, J.; Leigh, P.N.; et al. Consensus criteria for the diagnosis of frontotemporal cognitive and behavioural syndromes in amyotrophic lateral sclerosis. *Amyotroph. Lateral Scler.* **2009**, *10*, 131–146. [[CrossRef](#)]
- Rascovsky, K.; Hodges, J.R.; Knopman, D.; Mendez, M.F.; Kramer, J.H.; Neuhaus, J.; van Swieten, J.C.; Seelaar, H.; Dopper, E.G.P.; Onyike, C.U.; et al. Sensitivity of revised diagnostic criteria for the behavioural variant of frontotemporal dementia. *Brain A J. Neurol.* **2011**, *134*, 2456–2477. [[CrossRef](#)]
- Seelaar, H.; Rohrer, J.D.; Pijnenburg, Y.A.L.; Fox, N.C.; van Swieten, J.C. Clinical, genetic and pathological heterogeneity of frontotemporal dementia: A review. *J. Neurol. Neurosurg. Psychiatry* **2011**, *82*, 476–486. [[CrossRef](#)]
- Raaphorst, J.; De Visser, M.; Linssen, W.H.J.P.; De Haan, R.J.; Schmand, B. The cognitive profile of amyotrophic lateral sclerosis: A meta-analysis. *Amyotroph. Lateral Scler.* **2010**, *11*, 27–37. [[CrossRef](#)]
- Lomen-Hoerth, C.; Murphy, J.; Langmore, S.; Kramer, J.H.; Olney, R.K.; Miller, B. Are amyotrophic lateral sclerosis patients cognitively normal? *Neurology* **2003**, *60*, 1094–1097. [[CrossRef](#)]

10. Woolley, S.; Goetz, R.; Factor-Litvak, P.; Murphy, J.; Hupf, J.; Lomen-Hoerth, C.; Andrews, H.; Heitzman, D.; Bedlack, R.; Katz, J.; et al. Longitudinal Screening Detects Cognitive Stability and Behavioral Deterioration in ALS Patients. *Behav. Neurol.* **2018**, *2018*, 5969137. [[CrossRef](#)]
11. Woolley, S.C.; York, M.K.; Moore, D.H.; Strutt, A.M.; Murphy, J.; Schulz, P.E.; Katz, J.S. Detecting frontotemporal dysfunction in ALS: Utility of the ALS Cognitive Behavioral Screen (ALS-CBS). *Amyotroph. Lateral Scler. Off. Publ. World Fed. Neurol. Res. Group Mot. Neuron Dis.* **2010**, *11*, 303–311. [[CrossRef](#)] [[PubMed](#)]
12. Goldstein, L.H.; Abrahams, S. Changes in cognition and behaviour in amyotrophic lateral sclerosis: Nature of impairment and implications for assessment. *Lancet Neurol.* **2013**, *12*, 368–380. [[CrossRef](#)] [[PubMed](#)]
13. Geser, F.; Prvulovic, D.; O'Dwyer, L.; Hardiman, O.; Bede, P.; Bokde, A.L.; Trojanowski, J.Q.; Hampel, H. On the development of markers for pathological TDP-43 in amyotrophic lateral sclerosis with and without dementia. *Prog. Neurobiol.* **2011**, *95*, 649–662. [[CrossRef](#)] [[PubMed](#)]
14. DeJesus-Hernandez, M.; Mackenzie, I.R.; Boeve, B.F.; Boxer, A.L.; Baker, M.; Rutherford, N.J.; Nicholson, A.M.; Finch, N.A.; Flynn, H.; Adamson, J.; et al. Expanded GGGGCC hexanucleotide repeat in noncoding region of C9ORF72 causes chromosome 9p-linked FTD and ALS. *Neuron* **2011**, *72*, 245–256. [[CrossRef](#)]
15. Rohrer, J.D.; Isaacs, A.M.; Mizlienska, S.; Mead, S.; Lashley, T.; Wray, S.; Sidle, K.; Fratta, P.; Orrell, R.W.; Hardy, J.; et al. C9orf72 expansions in frontotemporal dementia and amyotrophic lateral sclerosis. *Lancet Neurol.* **2015**, *14*, 291–301. [[CrossRef](#)] [[PubMed](#)]
16. Abrahams, S.; Leigh, P.N.; Harvey, A.; Vythelingum, G.N.; Grise, D.; Goldstein, L.H. Verbal fluency and executive dysfunction in amyotrophic lateral sclerosis (ALS). *Neuropsychologia* **2000**, *38*, 734–747. [[CrossRef](#)]
17. Abrahams, S.; Goldstein, L.H.; Kew, J.J.; Brooks, D.J.; Lloyd, C.M.; Frith, C.D.; Leigh, P.N. Frontal lobe dysfunction in amyotrophic lateral sclerosis. A PET study. *Brain A J. Neurol.* **1996**, *119 Pt 6*, 2105–2120. [[CrossRef](#)]
18. Kew, J.J.; Goldstein, L.H.; Leigh, P.N.; Abrahams, S.; Cosgrave, N.; Passingham, R.E.; Frackowiak, R.S.; Brooks, D.J. The relationship between abnormalities of cognitive function and cerebral activation in amyotrophic lateral sclerosis. A neuropsychological and positron emission tomography study. *Brain A J. Neurol.* **1993**, *116 Pt 6*, 1399–1423. [[CrossRef](#)]
19. Hodges, J.R.; Mitchell, J.; Dawson, K.; Spillantini, M.G.; Xuereb, J.H.; McMonagle, P.; Nestor, P.J.; Patterson, K. Semantic dementia: Demography, familial factors and survival in a consecutive series of 100 cases. *Brain A J. Neurol.* **2010**, *133*, 300–306. [[CrossRef](#)] [[PubMed](#)]
20. Spinelli, E.G.; Ghirelli, A.; Basaia, S.; Cividini, C.; Riva, N.; Canu, E.; Castelnovo, V.; Domi, T.; Magnani, G.; Caso, F.; et al. Structural MRI Signatures in Genetic Presentations of the Frontotemporal Dementia/Motor Neuron Disease Spectrum. *Neurology* **2021**, *97*, e1594–e1607. [[CrossRef](#)]
21. Belder, C.R.S.; Chokesuwattanasakul, A.; Marshall, C.R.; Hardy, C.J.D.; Rohrer, J.D.; Warren, J.D. The problematic syndrome of right temporal lobe atrophy: Unweaving the phenotypic rainbow. *Front. Neurol.* **2022**, *13*, 1082828. [[CrossRef](#)] [[PubMed](#)]
22. Ulugut Erkoyun, H.; Groot, C.; Heilbron, R.; Nelissen, A.; van Rossum, J.; Jutten, R.; Koene, T.; van der Flier, W.M.; Wattjes, M.P.; Scheltens, P.; et al. A clinical-radiological framework of the right temporal variant of frontotemporal dementia. *Brain* **2020**, *143*, 2831–2843. [[CrossRef](#)] [[PubMed](#)]
23. Younes, K.; Borghesani, V.; Montembeault, M.; Spina, S.; Mandelli, M.L.; Welch, A.E.; Weis, E.; Callahan, P.; Elahi, F.M.; Hua, A.Y.; et al. Right temporal degeneration and socioemotional semantics: Semantic behavioural variant frontotemporal dementia. *Brain A J. Neurol.* **2022**, *145*, 4080–4096. [[CrossRef](#)] [[PubMed](#)]
24. Kumfor, F.; Landin-Romero, R.; Devenney, E.; Hutchings, R.; Grasso, R.; Hodges, J.R.; Piguet, O. On the right side? A longitudinal study of left- versus right-lateralized semantic dementia. *Brain* **2016**, *139*, 986–998. [[CrossRef](#)] [[PubMed](#)]
25. Seeley, W.W.; Bauer, A.M.; Miller, B.L.; Gorno-Tempini, M.L.; Kramer, J.H.; Weiner, M.; Rosen, H.J. The natural history of temporal variant frontotemporal dementia. *Neurology* **2005**, *64*, 1384–1390. [[CrossRef](#)]
26. Edwards-Lee, T.; Miller, B.L.; Benson, D.F.; Cummings, J.L.; Russell, G.L.; Boone, K.; Mena, I. The temporal variant of frontotemporal dementia. *Brain* **1997**, *120 Pt 6*, 1027–1040. [[CrossRef](#)] [[PubMed](#)]
27. Chan, D.; Anderson, V.; Pijnenburg, Y.; Whitwell, J.; Barnes, J.; Scahill, R.; Stevens, J.M.; Barkhof, F.; Scheltens, P.; Rossor, M.N.; et al. The clinical profile of right temporal lobe atrophy. *Brain* **2009**, *132*, 1287–1298. [[CrossRef](#)] [[PubMed](#)]
28. Abrahams, S.; Newton, J.; Niven, E.; Foley, J.; Bak, T.H. Screening for cognition and behaviour changes in ALS. *Amyotroph. Lateral Scler. Front. Degener.* **2014**, *15*, 9–14. [[CrossRef](#)] [[PubMed](#)]
29. Brooks, B.R.; Miller, R.G.; Swash, M.; Munsat, T.L.; Gr, W.F.N.R. El Escorial revisited: Revised criteria for the diagnosis of amyotrophic lateral sclerosis. *Amyotroph. Lateral Scler.* **2000**, *1*, 293–299. [[CrossRef](#)]
30. Douaud, G.; Smith, S.; Jenkinson, M.; Behrens, T.; Johansen-Berg, H.; Vickers, J.; James, S.; Voets, N.; Watkins, K.; Matthews, P.M.; et al. Anatomically related grey and white matter abnormalities in adolescent-onset schizophrenia. *Brain A J. Neurol.* **2007**, *130*, 2375–2386. [[CrossRef](#)]
31. Good, C.D.; Johnsrude, I.S.; Ashburner, J.; Henson, R.N.; Friston, K.J.; Frackowiak, R.S. A voxel-based morphometric study of ageing in 465 normal adult human brains. *NeuroImage* **2001**, *14*, 21–36. [[CrossRef](#)] [[PubMed](#)]
32. Smith, S.M.; Jenkinson, M.; Woolrich, M.W.; Beckmann, C.F.; Behrens, T.E.; Johansen-Berg, H.; Bannister, P.R.; De Luca, M.; Drobnjak, I.; Flitney, D.E.; et al. Advances in functional and structural MR image analysis and implementation as FSL. *NeuroImage* **2004**, *23* (Suppl. 1), S208–S219. [[CrossRef](#)] [[PubMed](#)]
33. Smith, S.M. Fast robust automated brain extraction. *Hum. Brain Mapp.* **2002**, *17*, 143–155. [[CrossRef](#)] [[PubMed](#)]

34. Winkler, A.M.; Ridgway, G.R.; Webster, M.A.; Smith, S.M.; Nichols, T.E. Permutation inference for the general linear model. *NeuroImage* **2014**, *92*, 381–397. [[CrossRef](#)]
35. Smith, S.M.; Nichols, T.E. Threshold-free cluster enhancement: Addressing problems of smoothing, threshold dependence and localisation in cluster inference. *NeuroImage* **2009**, *44*, 83–98. [[CrossRef](#)]
36. Smith, S.M.; Jenkinson, M.; Johansen-Berg, H.; Rueckert, D.; Nichols, T.E.; Mackay, C.E.; Watkins, K.E.; Ciccarelli, O.; Cader, M.Z.; Matthews, P.M.; et al. Tract-based spatial statistics: Voxelwise analysis of multi-subject diffusion data. *NeuroImage* **2006**, *31*, 1487–1505. [[CrossRef](#)]
37. Fischl, B. FreeSurfer. *NeuroImage* **2012**, *62*, 774–781. [[CrossRef](#)] [[PubMed](#)]
38. Fischl, B.; Dale, A.M. Measuring the thickness of the human cerebral cortex from magnetic resonance images. *Proc. Natl. Acad. Sci. USA* **2000**, *97*, 11050–11055. [[CrossRef](#)] [[PubMed](#)]
39. Fischl, B.; Salat, D.H.; Busa, E.; Albert, M.; Dieterich, M.; Haselgrove, C.; van der Kouwe, A.; Killiany, R.; Kennedy, D.; Klaveness, S.; et al. Whole brain segmentation: Automated labeling of neuroanatomical structures in the human brain. *Neuron* **2002**, *33*, 341–355. [[CrossRef](#)]
40. Buckner, R.L.; Head, D.; Parker, J.; Fotenos, A.F.; Marcus, D.; Morris, J.C.; Snyder, A.Z. A unified approach for morphometric and functional data analysis in young, old, and demented adults using automated atlas-based head size normalization: Reliability and validation against manual measurement of total intracranial volume. *NeuroImage* **2004**, *23*, 724–738. [[CrossRef](#)]
41. Turner, M.R.; Talbot, K. Sweet food preference in amyotrophic lateral sclerosis. *Pract. Neurol.* **2017**, *17*, 128–129. [[CrossRef](#)]
42. Sun, S.W.; Liang, H.F.; Trinkaus, K.; Cross, A.H.; Armstrong, R.C.; Song, S.K. Noninvasive detection of cuprizone induced axonal damage and demyelination in the mouse corpus callosum. *Magn. Reson. Med. Off. J. Soc. Magn. Reson. Med. Soc. Magn. Reson. Med.* **2006**, *55*, 302–308. [[CrossRef](#)]
43. Song, S.K.; Sun, S.W.; Ramsbottom, M.J.; Chang, C.; Russell, J.; Cross, A.H. Dysmyelination revealed through MRI as increased radial (but unchanged axial) diffusion of water. *NeuroImage* **2002**, *17*, 1429–1436. [[CrossRef](#)]
44. Neary, D.; Snowden, J.S.; Gustafson, L.; Passant, U.; Stuss, D.; Black, S.; Freedman, M.; Kertesz, A.; Robert, P.H.; Albert, M.; et al. Frontotemporal lobar degeneration. *Neurology* **1998**, *51*, 1546. [[CrossRef](#)]
45. Kamminga, J.; Kumfor, F.; Burrell, J.R.; Piguët, O.; Hodges, J.R.; Irish, M. Differentiating between right-lateralised semantic dementia and behavioural-variant frontotemporal dementia: An examination of clinical characteristics and emotion processing. *J. Neurol. Neurosurg. Psychiatry* **2015**, *86*, 1082–1088. [[CrossRef](#)] [[PubMed](#)]
46. Szaflarski, J.P.; Binder, J.R.; Possing, E.T.; McKiernan, K.A.; Ward, B.D.; Hammeke, T.A. Language lateralization in left-handed and ambidextrous people. *Neurology* **2002**, *59*, 238. [[CrossRef](#)] [[PubMed](#)]
47. Ghirelli, A.; Spinelli, E.G.; Canu, E.; Basaia, S.; Castelnovo, V.; Cecchetti, G.; Sibilla, E.; Domi, T.; Magnani, G.; Caso, F.; et al. Clinical and neuroanatomical characterization of the semantic behavioral variant of frontotemporal dementia in a multicenter Italian cohort. *J. Neurol.* **2024**, *271*, 4203–4215. [[CrossRef](#)] [[PubMed](#)]
48. Brambati, S.M.; Rankin, K.P.; Narvid, J.; Seeley, W.W.; Dean, D.; Rosen, H.J.; Miller, B.L.; Ashburner, J.; Gorno-Tempini, M.L. Atrophy progression in semantic dementia with asymmetric temporal involvement: A tensor-based morphometry study. *Neurobiol. Aging* **2009**, *30*, 103–111. [[CrossRef](#)]
49. Rosen, H.J.; Perry, R.J.; Murphy, J.; Kramer, J.H.; Mychack, P.; Schuff, N.; Weiner, M.; Levenson, R.W.; Miller, B.L. Emotion comprehension in the temporal variant of frontotemporal dementia. *Brain* **2002**, *125*, 2286–2295. [[CrossRef](#)]
50. Gainotti, G. Different patterns of famous people recognition disorders in patients with right and left anterior temporal lesions: A systematic review. *Neuropsychologia* **2007**, *45*, 1591–1607. [[CrossRef](#)]
51. Irish, M.; Kumfor, F.; Hodges, J.R.; Piguët, O. A tale of two hemispheres: Contrasting socioemotional dysfunction in right- versus left-lateralised semantic dementia. *Dement. Neuropsychol.* **2013**, *7*, 88–95. [[CrossRef](#)]
52. Rankin, K.P.; Gorno-Tempini, M.L.; Allison, S.C.; Stanley, C.M.; Glenn, S.; Weiner, M.W.; Miller, B.L. Structural anatomy of empathy in neurodegenerative disease. *Brain A J. Neurol.* **2006**, *129*, 2945–2956. [[CrossRef](#)]
53. Irish, M.; Hodges, J.R.; Piguët, O. Right anterior temporal lobe dysfunction underlies theory of mind impairments in semantic dementia. *Brain* **2014**, *137*, 1241–1253. [[CrossRef](#)]
54. Rankin, K.P.; Salazar, A.; Gorno-Tempini, M.L.; Sollberger, M.; Wilson, S.M.; Pavlic, D.; Stanley, C.M.; Glenn, S.; Weiner, M.W.; Miller, B.L. Detecting sarcasm from paralinguistic cues: Anatomic and cognitive correlates in neurodegenerative disease. *NeuroImage* **2009**, *47*, 2005–2015. [[CrossRef](#)]
55. Mendez, M.F.; McMurtray, A.; Chen, A.K.; Shapira, J.S.; Mishkin, F.; Miller, B.L. Functional neuroimaging and presenting psychiatric features in frontotemporal dementia. *J. Neurol. Neurosurg. Psychiatry* **2006**, *77*, 4–7. [[CrossRef](#)]
56. Ulugut, H.; Dijkstra, A.A.; Scarioni, M.; Barkhof, F.; Scheltens, P.; Rozemuller, A.J.M.; Pijnenburg, Y.A.L. Right temporal variant frontotemporal dementia is pathologically heterogeneous: A case-series and a systematic review. *Acta Neuropathol. Commun.* **2021**, *9*, 131. [[CrossRef](#)] [[PubMed](#)]
57. Josephs, K.A.; Whitwell, J.L.; Knopman, D.S.; Boeve, B.F.; Vemuri, P.; Senjem, M.L.; Parisi, J.E.; Ivnik, R.J.; Dickson, D.W.; Petersen, R.C.; et al. Two distinct subtypes of right temporal variant frontotemporal dementia. *Neurology* **2009**, *73*, 1443–1450. [[CrossRef](#)]
58. McKenna, M.C.; Corcia, P.; Couratier, P.; Siah, W.F.; Pradat, P.F.; Bede, P. Frontotemporal Pathology in Motor Neuron Disease Phenotypes: Insights From Neuroimaging. *Front. Neurol.* **2021**, *12*, 723450. [[CrossRef](#)] [[PubMed](#)]



59. McKenna, M.C.; Chipika, R.H.; Li Hi Shing, S.; Christidi, F.; Lope, J.; Doherty, M.A.; Hengeveld, J.C.; Vajda, A.; McLaughlin, R.L.; Hardiman, O.; et al. Infratentorial pathology in frontotemporal dementia: Cerebellar grey and white matter alterations in FTD phenotypes. *J. Neurol.* **2021**, *268*, 4687–4697. [[CrossRef](#)] [[PubMed](#)]
60. Abrahams, S.; Leigh, P.N.; Goldstein, L.H. Cognitive change in ALS—A prospective study. *Neurology* **2005**, *64*, 1222–1226. [[CrossRef](#)]
61. Costello, E.; Rooney, J.; Pinto-Grau, M.; Burke, T.; Elamin, M.; Bede, P.; McMackin, R.; Dukic, S.; Vajda, A.; Heverin, M.; et al. Cognitive reserve in amyotrophic lateral sclerosis (ALS): A population-based longitudinal study. *J. Neurol. Neurosurg. Psychiatry* **2021**, *92*, 460–465. [[CrossRef](#)] [[PubMed](#)]
62. Tahedl, M.; Li Hi Shing, S.; Finegan, E.; Chipika, R.H.; Lope, J.; Hardiman, O.; Bede, P. Propagation patterns in motor neuron diseases: Individual and phenotype-associated disease-burden trajectories across the UMN-LMN spectrum of MNDs. *Neurobiol. Aging* **2021**, *109*, 78–87. [[CrossRef](#)] [[PubMed](#)]
63. Bede, P.; Chipika, R.H.; Christidi, F.; Hengeveld, J.C.; Karavasilis, E.; Argyropoulos, G.D.; Lope, J.; Li Hi Shing, S.; Velonakis, G.; Dupuis, L.; et al. Genotype-associated cerebellar profiles in ALS: Focal cerebellar pathology and cerebro-cerebellar connectivity alterations. *J. Neurol. Neurosurg. Psychiatry* **2021**, *92*, 1197–1205. [[CrossRef](#)] [[PubMed](#)]
64. Finegan, E.; Hi Shing, S.L.; Chipika, R.H.; McKenna, M.C.; Doherty, M.A.; Hengeveld, J.C.; Vajda, A.; Donaghy, C.; McLaughlin, R.L.; Hutchinson, S.; et al. Thalamic, hippocampal and basal ganglia pathology in primary lateral sclerosis and amyotrophic lateral sclerosis: Evidence from quantitative imaging data. *Data Brief* **2020**, *29*, 105115. [[CrossRef](#)] [[PubMed](#)]
65. Abrahams, S.; Leigh, P.N.; Kew, J.J.; Goldstein, L.H.; Lloyd, C.M.; Brooks, D.J. A positron emission tomography study of frontal lobe function (verbal fluency) in amyotrophic lateral sclerosis. *J. Neurol. Sci.* **1995**, *129*, 44–46. [[CrossRef](#)] [[PubMed](#)]
66. Abrahams, S.; Goldstein, L.H.; Suckling, J.; Ng, V.; Simmons, A.; Chitnis, X.; Atkins, L.; Williams, S.C.R.; Leigh, P.N. Frontotemporal white matter changes in amyotrophic lateral sclerosis. *J. Neurol.* **2005**, *252*, 321–331. [[CrossRef](#)] [[PubMed](#)]
67. Pettit, L.D.; Bastin, M.E.; Smith, C.; Bak, T.H.; Gillingwater, T.H.; Abrahams, S. Executive deficits, not processing speed relates to abnormalities in distinct prefrontal tracts in amyotrophic lateral sclerosis. *Brain A J. Neurol.* **2013**, *136*, 3290–3304. [[CrossRef](#)]
68. Goldstein, L.H.; Newsom-Davis, I.C.; Bryant, V.; Brammer, M.; Leigh, P.N.; Simmons, A. Altered patterns of cortical activation in ALS patients during attention and cognitive response inhibition tasks. *J. Neurol.* **2011**, *258*, 2186–2198. [[CrossRef](#)]
69. Abrahams, S.; Goldstein, L.H.; Lloyd, C.M.; Brooks, D.J.; Leigh, P.N. Cognitive deficits in non-demented amyotrophic lateral sclerosis patients: A neuropsychological investigation. *J. Neurol. Sci.* **1995**, *129*, 54–55. [[CrossRef](#)]
70. Finegan, E.; Chipika, R.H.; Li Hi Shing, S.; Hardiman, O.; Bede, P. Pathological Crying and Laughing in Motor Neuron Disease: Pathobiology, Screening, Intervention. *Front. Neurol.* **2019**, *10*, 260. [[CrossRef](#)]
71. Burke, T.; Lonergan, K.; Pinto-Grau, M.; Elamin, M.; Bede, P.; Madden, C.; Hardiman, O.; Pender, N. Visual encoding, consolidation, and retrieval in amyotrophic lateral sclerosis: Executive function as a mediator, and predictor of performance. *Amyotroph. Lateral Scler. Front. Degener.* **2017**, *18*, 193–201. [[CrossRef](#)]
72. Burke, T.; Elamin, M.; Bede, P.; Pinto-Grau, M.; Lonergan, K.; Hardiman, O.; Pender, N. Discordant performance on the ‘Reading the Mind in the Eyes’ Test, based on disease onset in amyotrophic lateral sclerosis. *Amyotroph. Lateral Scler. Front. Degener.* **2016**, *17*, 467–472. [[CrossRef](#)]
73. Tahedl, M.; Tan, E.L.; Chipika, R.H.; Lope, J.; Hengeveld, J.C.; Doherty, M.A.; McLaughlin, R.L.; Hardiman, O.; Hutchinson, S.; McKenna, M.C.; et al. The involvement of language-associated networks, tracts, and cortical regions in frontotemporal dementia and amyotrophic lateral sclerosis: Structural and functional alterations. *Brain Behav.* **2023**, *13*, e3250. [[CrossRef](#)]
74. Radakovic, R.; Stephenson, L.; Colville, S.; Swingler, R.; Chandran, S.; Abrahams, S. Multidimensional apathy in ALS: Validation of the Dimensional Apathy Scale. *J. Neurol. Neurosurg. Psychiatry* **2016**, *87*, 663–669. [[CrossRef](#)]
75. Machts, J.; Bittner, V.; Kasper, E.; Schuster, C.; Prudlo, J.; Abdulla, S.; Kollwe, K.; Petri, S.; Dengler, R.; Heinze, H.J.; et al. Memory deficits in amyotrophic lateral sclerosis are not exclusively caused by executive dysfunction: A comparative neuropsychological study of amnesic mild cognitive impairment. *BMC Neurosci.* **2014**, *15*, 83. [[CrossRef](#)] [[PubMed](#)]
76. Bak, T.H.; Hodges, J.R. Motor neurone disease, dementia and aphasia: Coincidence, co-occurrence or continuum? *J. Neurol.* **2001**, *248*, 260–270. [[CrossRef](#)]
77. Taylor, L.J.; Brown, R.G.; Tsermentseli, S.; Al-Chalabi, A.; Shaw, C.E.; Ellis, C.M.; Leigh, P.N.; Goldstein, L.H. Is language impairment more common than executive dysfunction in amyotrophic lateral sclerosis? *J. Neurol. Neurosurg. Psychiatry* **2013**, *84*, 494–498. [[CrossRef](#)] [[PubMed](#)]
78. Woolley, S.C.; Zhang, Y.; Schuff, N.; Weiner, M.W.; Katz, J.S. Neuroanatomical correlates of apathy in ALS using 4 Tesla diffusion tensor MRI. *Amyotroph. Lateral Scler.* **2011**, *12*, 52–58. [[CrossRef](#)]
79. Olney, R.K.; Murphy, J.; Forshe, D.; Garwood, E.; Miller, B.L.; Langmore, S.; Kohn, M.A.; Lomen-Hoerth, C. The effects of executive and behavioral dysfunction on the course of ALS. *Neurology* **2005**, *65*, 1774–1777. [[CrossRef](#)]
80. Chio, A.; Ilardi, A.; Cammarosano, S.; Moglia, C.; Montuschi, A.; Calvo, A. Neurobehavioral dysfunction in ALS has a negative effect on outcome and use of PEG and NIV. *Neurology* **2012**, *78*, 1085–1089. [[CrossRef](#)]
81. Chio, A.; Vignola, A.; Mastro, E.; Giudici, A.D.; Iazzolino, B.; Calvo, A.; Moglia, C.; Montuschi, A. Neurobehavioral symptoms in ALS are negatively related to caregivers’ burden and quality of life. *Eur. J. Neurol.* **2010**, *17*, 1298–1303. [[CrossRef](#)]
82. Mavridis, I.N.; Pyrgelis, E.S. Nucleus accumbens changes in amyotrophic lateral sclerosis. *Am. J. Neurodegener. Dis.* **2023**, *12*, 85–88. [[PubMed](#)]

83. Christidi, F.; Argyropoulos, G.D.; Karavasilis, E.; Velonakis, G.; Zouvelou, V.; Kourtesis, P.; Pantoleon, V.; Tan, E.L.; Daponte, A.; Aristeidou, S.; et al. Hippocampal Metabolic Alterations in Amyotrophic Lateral Sclerosis: A Magnetic Resonance Spectroscopy Study. *Life* **2023**, *13*, 571. [[CrossRef](#)]
84. Chipika, R.H.; Christidi, F.; Finegan, E.; Li Hi Shing, S.; McKenna, M.C.; Chang, K.M.; Karavasilis, E.; Doherty, M.A.; Hengeveld, J.C.; Vajda, A.; et al. Amygdala pathology in amyotrophic lateral sclerosis and primary lateral sclerosis. *J. Neurol. Sci.* **2020**, *417*, 117039. [[CrossRef](#)]
85. Anderson, V.E.; Cairns, N.J.; Leigh, P.N. Involvement of the amygdala, dentate and hippocampus in motor neuron disease. *J. Neurol. Sci.* **1995**, *129*, 75–78. [[CrossRef](#)]
86. Chipika, R.H.; Finegan, E.; Li Hi Shing, S.; McKenna, M.C.; Christidi, F.; Chang, K.M.; Doherty, M.A.; Hengeveld, J.C.; Vajda, A.; Pender, N.; et al. “Switchboard” malfunction in motor neuron diseases: Selective pathology of thalamic nuclei in amyotrophic lateral sclerosis and primary lateral sclerosis. *NeuroImage Clin.* **2020**, *27*, 102300. [[CrossRef](#)] [[PubMed](#)]
87. Chio, A.; Pagani, M.; Agosta, F.; Calvo, A.; Cistaro, A.; Filippi, M. Neuroimaging in amyotrophic lateral sclerosis: Insights into structural and functional changes. *Lancet Neurol.* **2014**, *13*, 1228–1240. [[CrossRef](#)] [[PubMed](#)]
88. Bonelli, R.M.; Cummings, J.L. Frontal-subcortical circuitry and behavior. *Dialogues Clin. Neurosci.* **2007**, *9*, 141–151. [[CrossRef](#)] [[PubMed](#)]
89. O’Callaghan, C.; Bertoux, M.; Hornberger, M. Beyond and below the cortex: The contribution of striatal dysfunction to cognition and behaviour in neurodegeneration. *J. Neurol. Neurosurg. Psychiatry* **2013**, *85*, 371–378. [[CrossRef](#)]
90. Meier, J.M.; van der Burgh, H.K.; Nitert, A.D.; Bede, P.; de Lange, S.C.; Hardiman, O.; van den Berg, L.H.; van den Heuvel, M.P. Connectome-Based Propagation Model in Amyotrophic Lateral Sclerosis. *Ann. Neurol.* **2020**, *87*, 725–738. [[CrossRef](#)]
91. Dukic, S.; McMackin, R.; Costello, E.; Metzger, M.; Buxo, T.; Fasano, A.; Chipika, R.; Pinto-Grau, M.; Schuster, C.; Hammond, M.; et al. Resting-state EEG reveals four subphenotypes of amyotrophic lateral sclerosis. *Brain A J. Neurol.* **2022**, *145*, 621–631. [[CrossRef](#)] [[PubMed](#)]
92. Bocchetta, M.; Gordon, E.; Cardoso, M.J.; Modat, M.; Ourselin, S.; Warren, J.D.; Rohrer, J.D. Thalamic atrophy in frontotemporal dementia—Not just a C9orf72 problem. *NeuroImage Clin.* **2018**, *18*, 675–681. [[CrossRef](#)] [[PubMed](#)]
93. Bocchetta, M.; Todd, E.G.; Peakman, G.; Cash, D.M.; Convery, R.S.; Russell, L.L.; Thomas, D.L.; Eugenio Iglesias, J.; van Swieten, J.C.; Jiskoot, L.C.; et al. Differential early subcortical involvement in genetic FTD within the GENFI cohort. *NeuroImage Clin.* **2021**, *30*, 102646. [[CrossRef](#)] [[PubMed](#)]
94. McKenna, M.C.; Li Hi Shing, S.; Murad, A.; Lope, J.; Hardiman, O.; Hutchinson, S.; Bede, P. Focal thalamus pathology in frontotemporal dementia: Phenotype-associated thalamic profiles. *J. Neurol. Sci.* **2022**, *436*, 120221. [[CrossRef](#)]
95. McKenna, M.C.; Lope, J.; Bede, P.; Tan, E.L. Thalamic pathology in frontotemporal dementia: Predilection for specific nuclei, phenotype-specific signatures, clinical correlates, and practical relevance. *Brain Behav.* **2023**, *13*, e2881. [[CrossRef](#)]
96. Finegan, E.; Li Hi Shing, S.; Chipika, R.H.; Doherty, M.A.; Hengeveld, J.C.; Vajda, A.; Donaghy, C.; Pender, N.; McLaughlin, R.L.; Hardiman, O.; et al. Widespread subcortical grey matter degeneration in primary lateral sclerosis: A multimodal imaging study with genetic profiling. *NeuroImage Clin.* **2019**, *24*, 102089. [[CrossRef](#)]
97. Finegan, E.; Shing, S.L.H.; Chipika, R.H.; Chang, K.M.; McKenna, M.C.; Doherty, M.A.; Hengeveld, J.C.; Vajda, A.; Pender, N.; Donaghy, C.; et al. Extra-motor cerebral changes and manifestations in primary lateral sclerosis. *Brain Imaging Behav.* **2021**, *15*, 2283–2296. [[CrossRef](#)]
98. Bertrand, A.; Wen, J.; Rinaldi, D.; Houot, M.; Sayah, S.; Camuzat, A.; Fournier, C.; Fontanella, S.; Routier, A.; Couratier, P.; et al. Early Cognitive, Structural, and Microstructural Changes in Presymptomatic C9orf72 Carriers Younger Than 40 Years. *JAMA Neurol.* **2018**, *75*, 236–245. [[CrossRef](#)]
99. Bede, P.; Lulé, D.; Müller, H.P.; Tan, E.L.; Dorst, J.; Ludolph, A.C.; Kassubek, J. Presymptomatic grey matter alterations in ALS kindreds: A computational neuroimaging study of asymptomatic C9orf72 and SOD1 mutation carriers. *J. Neurol.* **2023**, *270*, 4235–4247. [[CrossRef](#)]
100. Chipika, R.H.; Siah, W.F.; McKenna, M.C.; Li Hi Shing, S.; Hardiman, O.; Bede, P. The presymptomatic phase of amyotrophic lateral sclerosis: Are we merely scratching the surface? *J. Neurol.* **2021**, *268*, 4607–4629. [[CrossRef](#)]
101. Westeneng, H.J.; Walhout, R.; Straathof, M.; Schmidt, R.; Hendrikse, J.; Veldink, J.H.; van den Heuvel, M.P.; van den Berg, L.H. Widespread structural brain involvement in ALS is not limited to the C9orf72 repeat expansion. *J. Neurol. Neurosurg. Psychiatry* **2016**, *87*, 1354–1360. [[CrossRef](#)] [[PubMed](#)]
102. Li Hi Shing, S.; McKenna, M.C.; Siah, W.F.; Chipika, R.H.; Hardiman, O.; Bede, P. The imaging signature of C9orf72 hexanucleotide repeat expansions: Implications for clinical trials and therapy development. *Brain Imaging Behav.* **2021**, *15*, 2693–2719. [[CrossRef](#)] [[PubMed](#)]
103. van de Pol, L.A.; Hensel, A.; van der Flier, W.M.; Visser, P.J.; Pijnenburg, Y.A.; Barkhof, F.; Gertz, H.J.; Scheltens, P. Hippocampal atrophy on MRI in frontotemporal lobar degeneration and Alzheimer’s disease. *J. Neurol. Neurosurg. Psychiatry* **2006**, *77*, 439–442. [[CrossRef](#)] [[PubMed](#)]
104. Christidi, F.; Karavasilis, E.; Velonakis, G.; Ferentinos, P.; Rentzos, M.; Kelekis, N.; Evdokimidis, I.; Bede, P. The Clinical and Radiological Spectrum of Hippocampal Pathology in Amyotrophic Lateral Sclerosis. *Front. Neurol.* **2018**, *9*, 523. [[CrossRef](#)] [[PubMed](#)]

105. Trojsi, F.; Di Nardo, F.; Caiazzo, G.; Siciliano, M.; D'Alvano, G.; Ferrantino, T.; Passaniti, C.; Ricciardi, D.; Esposito, S.; Lavorgna, L.; et al. Hippocampal connectivity in Amyotrophic Lateral Sclerosis (ALS): More than Papez circuit impairment. *Brain Imaging Behav.* **2020**, *15*, 2126–2138. [[CrossRef](#)]
106. Bueno, A.P.A.; de Souza, L.C.; Pinaya, W.H.L.; Teixeira, A.L.; de Prado, L.G.R.; Caramelli, P.; Hornberger, M.; Sato, J.R. Papez Circuit Gray Matter and Episodic Memory in Amyotrophic Lateral Sclerosis and Behavioural Variant Frontotemporal Dementia. *Brain Imaging Behav.* **2021**, *15*, 996–1006. [[CrossRef](#)] [[PubMed](#)]
107. Bueno, A.P.A.; Pinaya, W.H.L.; Moura, L.M.; Bertoux, M.; Radakovic, R.; Kiernan, M.C.; Teixeira, A.L.; de Souza, L.C.; Hornberger, M.; Sato, J.R. Structural and functional papez circuit integrity in amyotrophic lateral sclerosis. *Brain Imaging Behav.* **2018**, *12*, 1622–1630. [[CrossRef](#)]
108. Horne, K.; Ahmed, R.M.; Pigué, O.; Irish, M. Establishing the link between motivational disturbances and behavioural rigidity in frontotemporal dementia. *Eur. J. Neurol.* **2024**, *31*, e16132. [[CrossRef](#)]
109. Barritt, A.W.; Gabel, M.C.; Cercignani, M.; Leigh, P.N. Emerging Magnetic Resonance Imaging Techniques and Analysis Methods in Amyotrophic Lateral Sclerosis. *Front. Neurol.* **2018**, *9*, 1065. [[CrossRef](#)]
110. Tahedl, M.; Tan, E.L.; Kleinerova, J.; Delaney, S.; Hengeveld, J.C.; Doherty, M.A.; McLaughlin, R.L.; Pradat, P.F.; Raoul, C.; Ango, F.; et al. Progressive Cerebrocerebellar Uncoupling in Sporadic and Genetic Forms of Amyotrophic Lateral Sclerosis. *Neurology* **2024**, *103*, e209623. [[CrossRef](#)]
111. Bede, P.; Murad, A.; Lope, J.; Li Hi Shing, S.; Finegan, E.; Chipika, R.H.; Hardiman, O.; Chang, K.M. Phenotypic categorisation of individual subjects with motor neuron disease based on radiological disease burden patterns: A machine-learning approach. *J. Neurol. Sci.* **2021**, *432*, 120079. [[CrossRef](#)] [[PubMed](#)]
112. Bede, P.; Murad, A.; Hardiman, O. Pathological neural networks and artificial neural networks in ALS: Diagnostic classification based on pathognomonic neuroimaging features. *J. Neurol.* **2021**, *269*, 2440–2452. [[CrossRef](#)] [[PubMed](#)]
113. Behler, A.; Müller, H.P.; Ludolph, A.C.; Lulé, D.; Kassubek, J. A multivariate Bayesian classification algorithm for cerebral stage prediction by diffusion tensor imaging in amyotrophic lateral sclerosis. *NeuroImage Clin.* **2022**, *35*, 103094. [[CrossRef](#)] [[PubMed](#)]
114. McCarthy, J.; Borroni, B.; Sanchez-Valle, R.; Moreno, F.; Laforce, R., Jr.; Graff, C.; Synofzik, M.; Galimberti, D.; Rowe, J.B.; Masellis, M.; et al. Data-driven staging of genetic frontotemporal dementia using multi-modal MRI. *Hum. Brain Mapp.* **2022**, *43*, 1821–1835. [[CrossRef](#)] [[PubMed](#)]
115. Chagué, P.; Marro, B.; Fadili, S.; Houot, M.; Morin, A.; Samper-González, J.; Beunon, P.; Arrivé, L.; Dormont, D.; Dubois, B.; et al. Radiological classification of dementia from anatomical MRI assisted by machine learning-derived maps. *J. Neuroradiol.* **2021**, *48*, 412–418. [[CrossRef](#)] [[PubMed](#)]
116. Kim, J.P.; Kim, J.; Park, Y.H.; Park, S.B.; Lee, J.S.; Yoo, S.; Kim, E.J.; Kim, H.J.; Na, D.L.; Brown, J.A.; et al. Machine learning based hierarchical classification of frontotemporal dementia and Alzheimer's disease. *NeuroImage Clin.* **2019**, *23*, 101811. [[CrossRef](#)] [[PubMed](#)]
117. Tahedl, M.; Murad, A.; Lope, J.; Hardiman, O.; Bede, P. Evaluation and categorisation of individual patients based on white matter profiles: Single-patient diffusion data interpretation in neurodegeneration. *J. Neurol. Sci.* **2021**, *428*, 117584. [[CrossRef](#)] [[PubMed](#)]
118. McKenna, M.C.; Tahedl, M.; Lope, J.; Chipika, R.H.; Li Hi Shing, S.; Doherty, M.A.; Hengeveld, J.C.; Vajda, A.; McLaughlin, R.L.; Hardiman, O.; et al. Mapping cortical disease-burden at individual-level in frontotemporal dementia: Implications for clinical care and pharmacological trials. *Brain Imaging Behav.* **2021**, *16*, 1196–1207. [[CrossRef](#)] [[PubMed](#)]
119. McKenna, M.C.; Tahedl, M.; Murad, A.; Lope, J.; Hardiman, O.; Hutchinson, S.; Bede, P. White matter microstructure alterations in frontotemporal dementia: Phenotype-associated signatures and single-subject interpretation. *Brain Behav.* **2022**, *12*, e2500. [[CrossRef](#)] [[PubMed](#)]
120. Tahedl, M.; Chipika, R.H.; Lope, J.; Li Hi Shing, S.; Hardiman, O.; Bede, P. Cortical progression patterns in individual ALS patients across multiple timepoints: A mosaic-based approach for clinical use. *J. Neurol.* **2021**, *268*, 1913–1926. [[CrossRef](#)]
121. McKenna, M.C.; Murad, A.; Huynh, W.; Lope, J.; Bede, P. The changing landscape of neuroimaging in frontotemporal lobar degeneration: From group-level observations to single-subject data interpretation. *Expert Rev. Neurother.* **2022**, *22*, 179–207. [[CrossRef](#)] [[PubMed](#)]
122. Pradat, P.F.; Bernard, E.; Corcia, P.; Couratier, P.; Jublanc, C.; Querin, G.; Morelot Panzini, C.; Salachas, F.; Vial, C.; Wahbi, K.; et al. The French national protocol for Kennedy's disease (SBMA): Consensus diagnostic and management recommendations. *Orphanet J. Rare Dis.* **2020**, *15*, 90. [[CrossRef](#)] [[PubMed](#)]
123. Querin, G.; Bede, P.; Marchand-Pauvert, V.; Pradat, P.F. Biomarkers of Spinal and Bulbar Muscle Atrophy (SBMA): A Comprehensive Review. *Front. Neurol.* **2018**, *9*, 844. [[CrossRef](#)]
124. Mulkerrin, G.; França, M.C., Jr.; Lope, J.; Tan, E.L.; Bede, P. Neuroimaging in hereditary spastic paraplegias: From qualitative cues to precision biomarkers. *Expert Rev. Mol. Diagn.* **2022**, *22*, 745–760. [[CrossRef](#)] [[PubMed](#)]
125. Di Napoli, J.; Arighi, A.; Conte, G.; Carandini, T.; Sacchi, L.; Arcaro, M.; Fenoglio, C.; Sorrentino, F.; Mercurio, M.; Pietroboni, A.M.; et al. Predominant right temporal lobe atrophy: Clinical, neuropsychological and structural differences based on amyloid status. *Eur. J. Neurol.* **2024**, *31*, e16124. [[CrossRef](#)]
126. Frings, L.; Blazhenets, G.; Binder, R.; Bormann, T.; Hellwig, S.; Meyer, P.T. More extensive hypometabolism and higher mortality risk in patients with right- than left-predominant neurodegeneration of the anterior temporal lobe. *Alzheimer's Res. Ther.* **2023**, *15*, 11. [[CrossRef](#)]

127. Luzzi, S.; Baldinelli, S.; Ranaldi, V.; Fabi, K.; Cafazzo, V.; Fringuelli, F.; Silvestrini, M.; Provinciali, L.; Reverberi, C.; Gainotti, G. Famous faces and voices: Differential profiles in early right and left semantic dementia and in Alzheimer's disease. *Neuropsychologia* **2017**, *94*, 118–128. [[CrossRef](#)]
128. Nelissen, N.; Dupont, P.; Vandebulcke, M.; Tousseyn, T.; Peeters, R.; Vandenberghe, R. Right hemisphere recruitment during language processing in frontotemporal lobar degeneration and Alzheimer's disease. *J. Mol. Neurosci. MN* **2011**, *45*, 637–647. [[CrossRef](#)]
129. Gasca-Salas, C.; Clavero, P.; García-García, D.; Obeso, J.A.; Rodríguez-Oroz, M.C. Significance of visual hallucinations and cerebral hypometabolism in the risk of dementia in Parkinson's disease patients with mild cognitive impairment. *Hum. Brain Mapp.* **2016**, *37*, 968–977. [[CrossRef](#)]
130. Zhai, H.; Fan, W.; Xiao, Y.; Zhu, Z.; Ding, Y.; He, C.; Zhang, W.; Xu, Y.; Zhang, Y. Voxel-based morphometry of grey matter structures in Parkinson's Disease with wearing-off. *Brain Imaging Behav.* **2023**, *17*, 725–737. [[CrossRef](#)]

**Disclaimer/Publisher's Note:** The statements, opinions and data contained in all publications are solely those of the individual author(s) and contributor(s) and not of MDPI and/or the editor(s). MDPI and/or the editor(s) disclaim responsibility for any injury to people or property resulting from any ideas, methods, instructions or products referred to in the content.